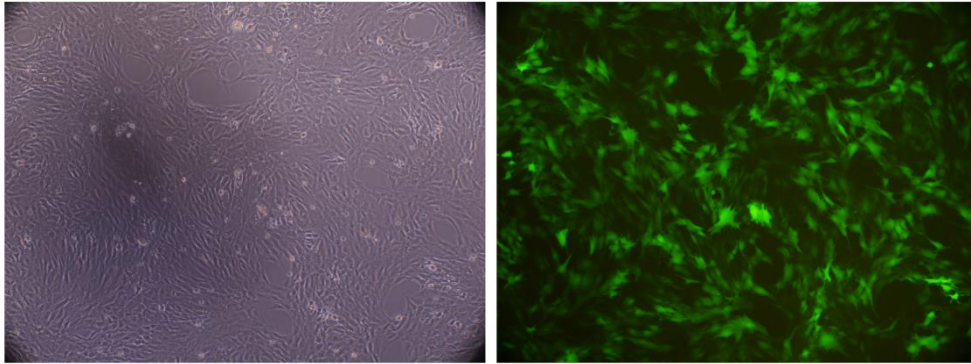


**Table S1**

	forward primer (5'→3')	reverse primer (5'→3')
CCL3	GCAGCGAGTACCAGTCCCTT	ACTTCGTTCCAGAGCGCCAT
CCL4	CTGCCTTCTCTCTCCTCCTG	AGGGTCAGAGCCTATTGGTG
IRF-1	TCTCTGATCAACACCTCTCAGCA	CATACTTGCTAAGGTTCTGTCCAG
IRF-6	ATCTCTGATCATCTCAGCACTACA	TCTGTCCAGCATACTTGCTAAGGT
IRF-7	TCTGGATGAAGCTGATGCAC	AGAGCTGGGCCAGTTGTAGA
IRF-8	AGCAGGGTGGTTCTGTGCTT	GCTGCTCTACCTGCACCAGA

**Table S1. Primers for CCL3/4 and IRF-1/6/7/8 mRNA detection.** Six pairs of primers were designed to amplify rat CCL3/4 and IRF-1/6/7/8 mRNA. The sequence of these primers was shown.

**Figure S1**

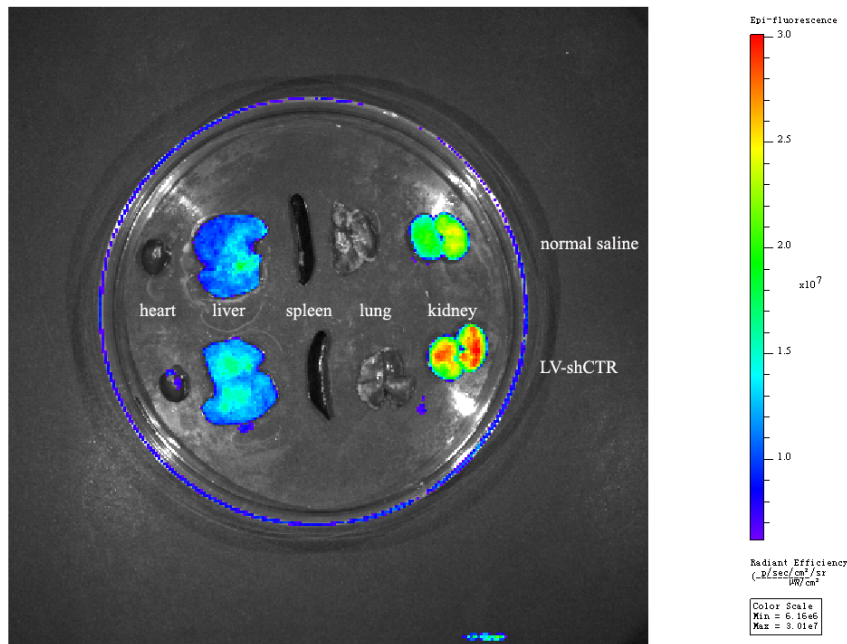


**Figure S1. Transfection efficiency of shRNA expression plasmids into rat GMCs.**

Transient transfection of shCTR expression plasmids into the cultured GMCs was conducted with Neon<sup>TM</sup> transfection system according to the manufacturer's procedure. The transfection efficiency of shRNA plasmids was detected by GFP at 48 h after transfection (right), and meanwhile, the same visual field were observed under ordinary light (left). The transfection efficiency was 80%~90% by counting the ratio of GFP expressing cells to total cells. The representative images were displayed (Magnification:  $\times 100$ ).

**Figure S2**

**A**



**B**

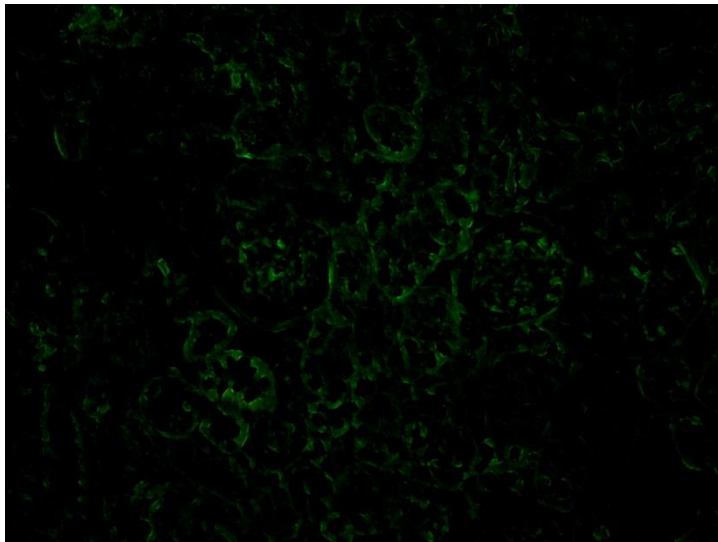


**Figure S2. Transfection efficiency of LV-shRNA *in vivo*.** The LV-shCTR was transfected into rat kidneys via renal artery perfusion suddenly followed by renal veins occlusion for 10 minutes. (A) At 96 h after perfusion, EGFP expression in different organs was examined by Caliper IVIS imaging system. (B) GFP expression in glomeruli and renal tubules was seen under a fluorescence microscope (Frozen sections, Magnification:  $\times 100$ ). The representative pictures were shown.

**Figure S3**

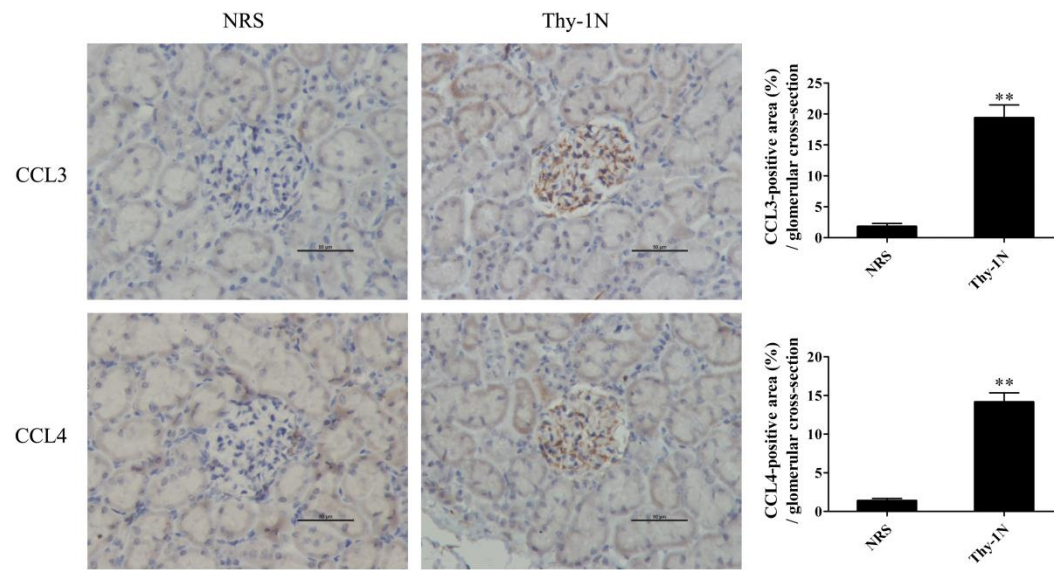


**Figure S3. CCL3/4 expression in the renal tissues of rats.** The protein levels of CCL3/4 in the renal tissues of Thy-1N and NRS rats at 6 h were examined by IHC staining (Magnification,  $\times 400$ ). \*\*  $P < 0.01$  vs. NRS group. Data were represented as means  $\pm$  SE ( $n=5$  in each group).

**Figure S4**

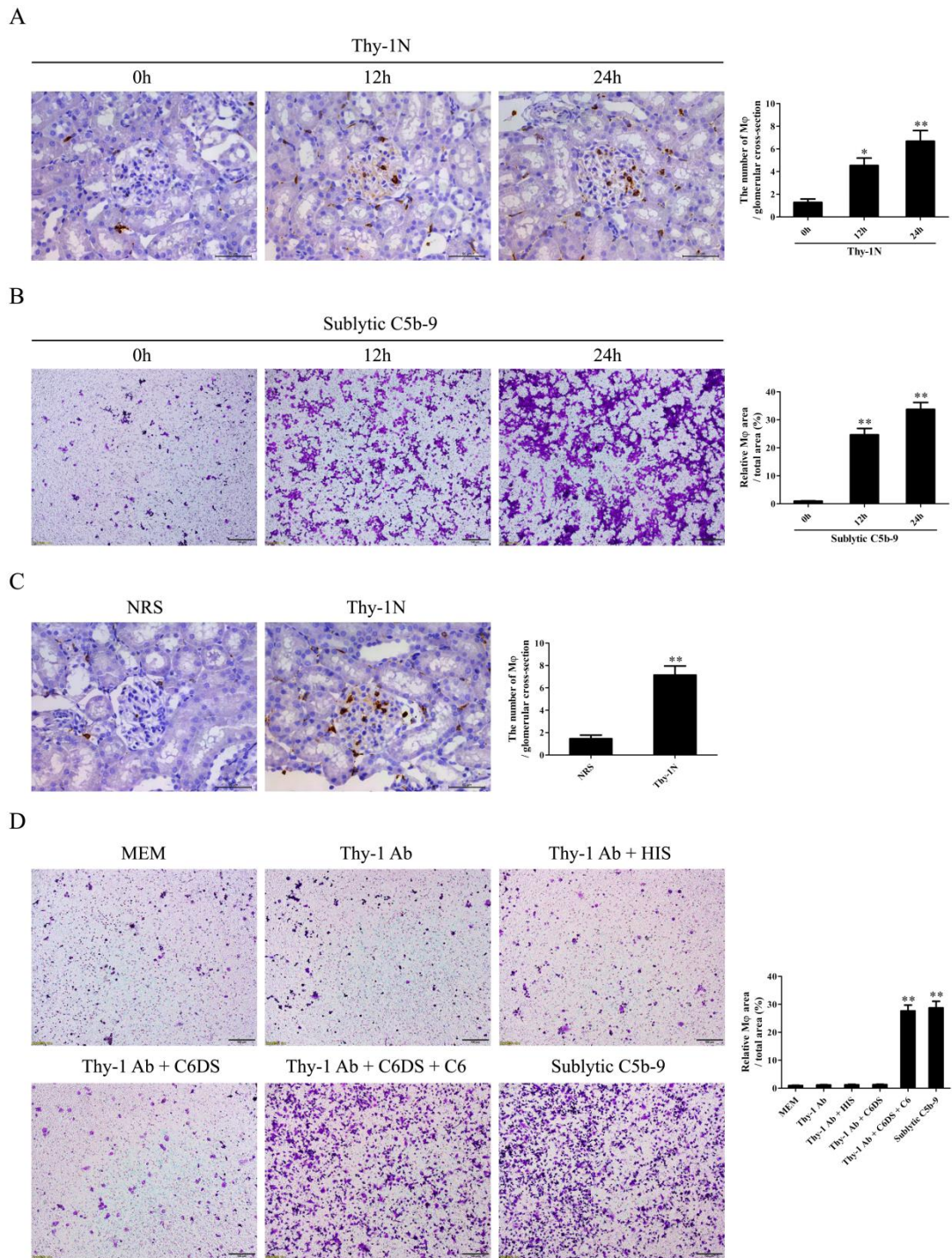
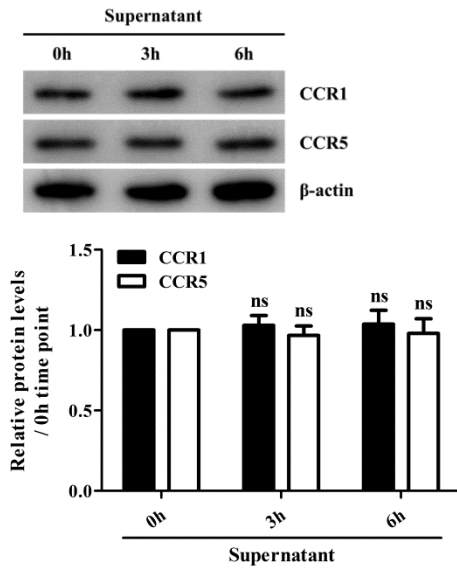


**Figure S4. M $\phi$  distribution in the renal tissues of Thy-1N rats and M $\phi$  chemotaxis induced by GMCs exposed to sublytic C5b-9.** (A) CD68<sup>+</sup> cell (M $\phi$ ) in the renal tissues of Thy-1N rats at 0 h, 12 h and 24 h was examined by IHC staining with anti-CD68 antibody (Magnification:  $\times 400$ ). \* P<0.05, \*\* P<0.01 vs. 0h. (B) An upper chamber containing M $\phi$

was separated by a membrane from a lower chamber containing GMCs following sublytic C5b-9 treatment for 0 h, 12 h and 24 h. Chemotaxis of M $\phi$  from the upper chamber into the lower chamber was observed by crystal violet staining of the membrane (Magnification:  $\times 100$ ). \*\* P<0.01 vs. 0h. (C) M $\phi$  in the renal tissues of Thy-1N rats and NRS rats at 24 h was observed by IHC staining with anti-CD68 antibody (Magnification:  $\times 400$ ). \*\* P<0.01 vs. NRS group. (D) An upper chamber containing M $\phi$  was separated by a membrane from a lower chamber containing GMCs. GMCs were divided into different groups of MEM, Thy-1 Ab, Thy-1 Ab + HIS, Thy-1 Ab + C6DS, Thy-1 Ab + C6DS + C6 and sublytic C5b-9 (Thy-1 Ab + NHS) respectively. Chemotaxis of M $\phi$  from the upper chamber into the lower chamber was observed by crystal violet staining of the membrane at 24 h after grouping treatment (Magnification:  $\times 100$ ). \*\* P<0.01 vs. other groups. Data were represented as means  $\pm$  SE (n=5).

**Figure S5**

**A**



**B**

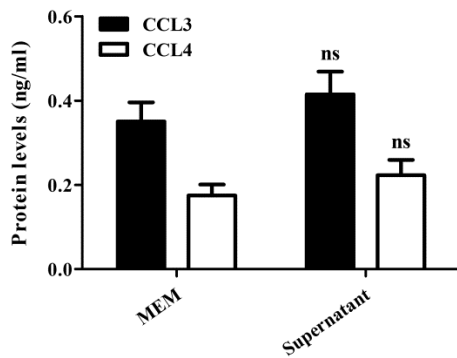


**Figure S5. The expression or secretion of CCR1/5 and CCL3/4 in  $M\phi$  with the stimulation of supernatant from the GMCs induced by sublytic C5b-9.** The GMCs were stimulated with sublytic C5b-9, and the supernatant was obtained after six hours.  $M\phi$  were incubated with the supernatant for 10 min, and changed to normal medium for continuous culture for 3 h and 6 h, and the expression of CCR1/5 and secretion of CCL3/4 were determined by IB (A, 3 h and 6 h) and ELISA (B, 6 h). Data were represented as means  $\pm$  SE ( $n=3$  in each group). <sup>ns</sup>  $P > 0.05$  vs. 0 h time point or MEM group.

**Figure S6**

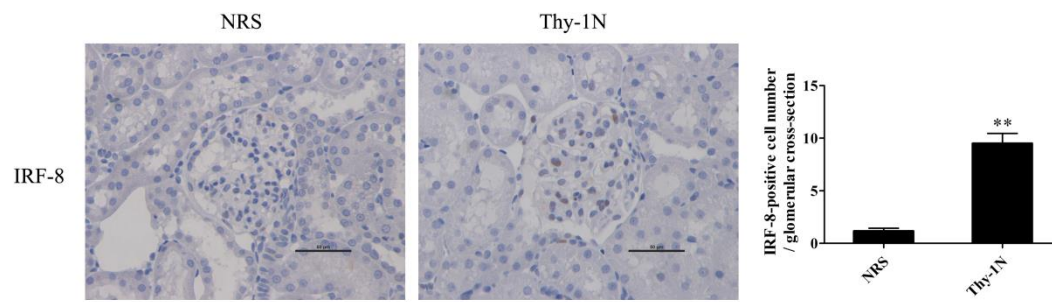


**Figure S6. IRF-8 expression in the renal tissues of rats.** The protein expression of IRF-8 in the renal tissues of Thy-1N and NRS rats at 3 h was examined by IHC staining (Magnification,  $\times 400$ ). \*\*  $P < 0.01$  vs. NRS group. Data were represented as means  $\pm$  SE (n=5 in each group).



**Figure S7**

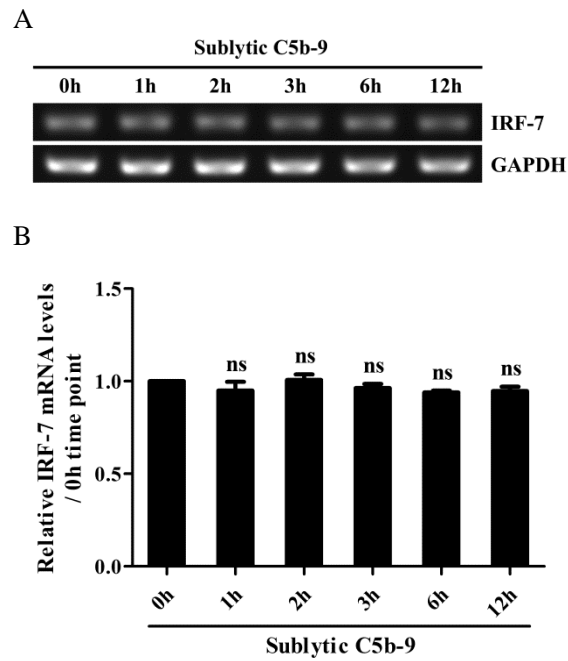
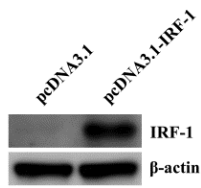


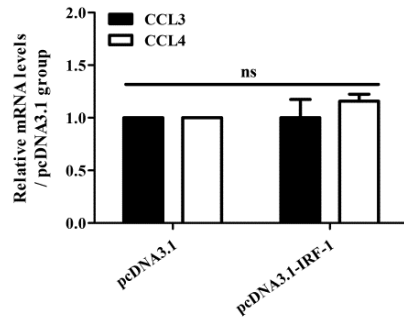
**Figure S7. IRF-7 expression in the GMCs exposed to sublytic C5b-9.** Rat GMCs were stimulated with sublytic C5b-9 for different time points, and then the mRNA levels of IRF-7 and GAPDH were detected by RT-PCR. Data were represented as means  $\pm$  SE (n=3 in each group). <sup>ns</sup> P>0.05 vs. 0 h time point.

**Figure S8**

A



B



C

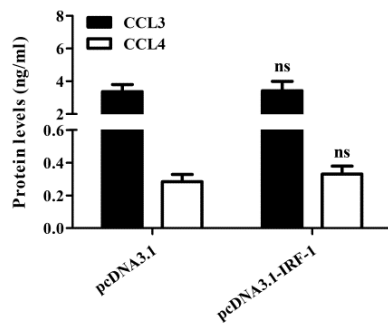


**Figure S8. The effect of IRF-1 overexpression on CCL3/4 production in the GMCs.** Rat GMCs were transfected with pcDNA3.1-IRF-1 or pcDNA3.1 for 48 h, and then the expression levels of IRF-1 and CCL3/4 in the GMCs were detected by IB (A), qPCR (B) and ELISA (C). Data were represented as means  $\pm$  SE (n=3). <sup>ns</sup> P>0.05 vs. pcDNA3.1 group.

**Figure S9**

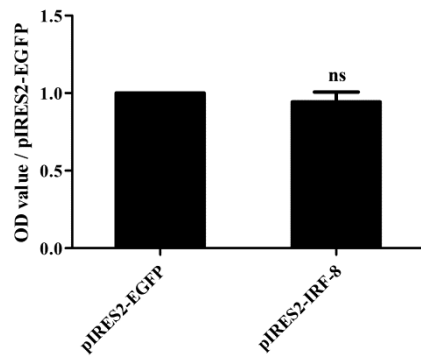


**Figure S9. The effect of IRF-8 overexpression on GMC proliferation.** Rat GMCs were transfected with pIRES2-IRF-8 and pIRES2-EGFP for 48 h, and the cellular proliferation was detected by CCK-8 assay. Data were represented as means  $\pm$  SE (n=3). <sup>ns</sup> P>0.05 vs. pIRES2-EGFP group.

**Figure S10**

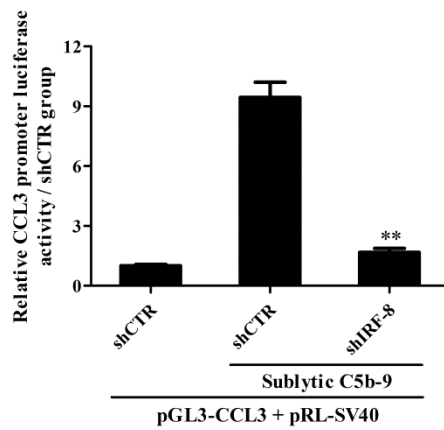
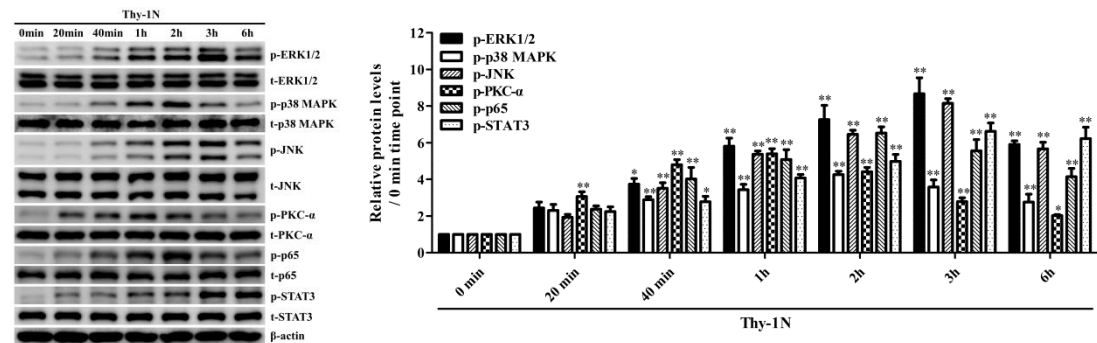


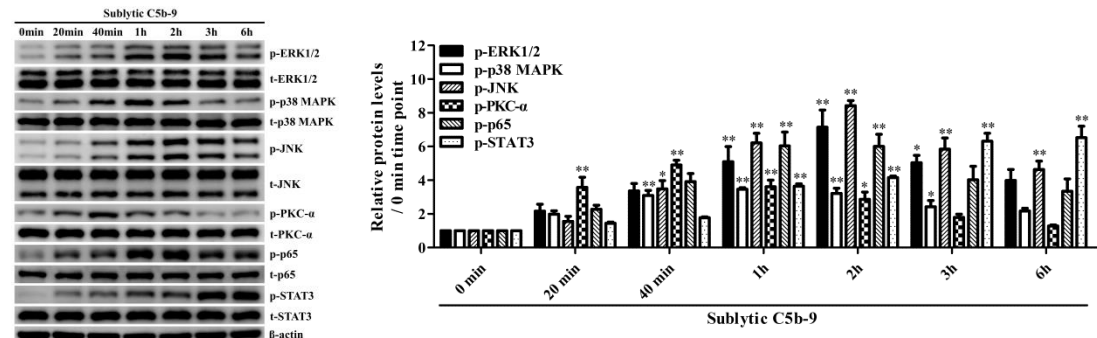
**Figure S10. The effect of IRF-8 knockdown on CCL3 gene transcription in the GMCs induced by sublytic C5b-9.** The plasmids of shIRF-8, shCTR, pGL3-CCL3 and pRL-SV40 were co-transfected into rat GMCs for 48 h in different groups followed by sublytic C5b-9 stimulation for 3 h, and then the luciferase activity was detected. Data were represented as means  $\pm$  SE (n=3). \*\* P<0.01 vs. shCTR + sublytic C5b-9.

**Figure S11**

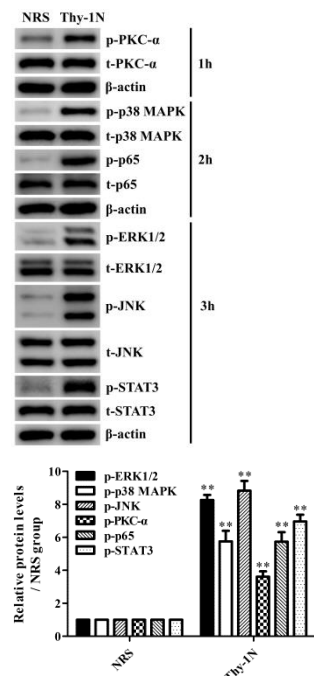
**A**



**B**



**C**



**D**

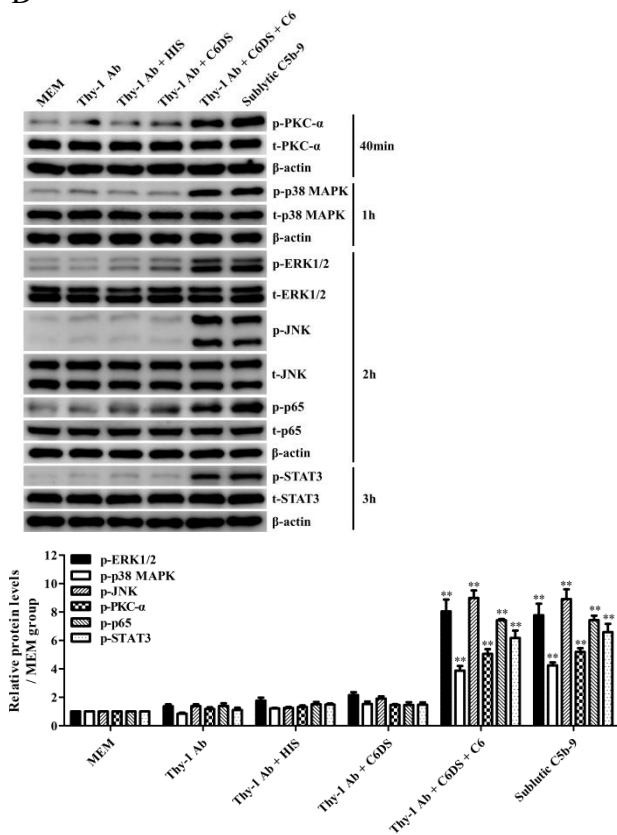


**Figure S11. The expression and phosphorylation of ERK1/2, p38 MAPK, JNK, PKC- $\alpha$ , p65 and STAT3 *in vivo* and *in vitro*.** (A and B) The expression and phosphorylation levels of ERK1/2, p38 MAPK, JNK, PKC- $\alpha$ , p65 and STAT3 in the renal tissues of Thy-1N rats (A) and in the GMCs exposed to sublytic C5b-9 (B) for different time was examined by IB. \* P<0.05, \*\* P<0.01 vs. 0h. (C) The expression levels of above-mentioned proteins in the renal tissues of Thy-1N and NRS rats at 1 h, 2 h or 3 h were examined by IB. \*\* P<0.01 vs. NRS group. (D) Rat GMCs were divided into different groups. At 40 min, 1 h, 2 h or 3 h after treatment, the expression levels of above-mentioned proteins were determined by IB. \*\* P<0.01 vs. other groups. Data were represented as means  $\pm$  SE (n=5 *in vivo*, n=3 *in vitro*).

**Figure S12**

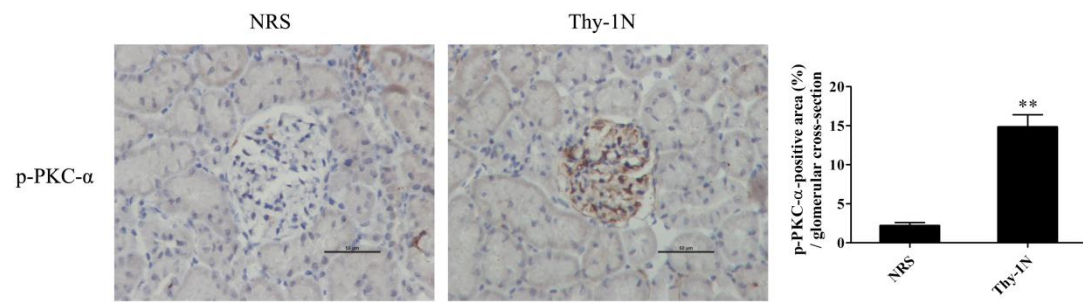


**Figure S12. The phosphorylation of PKC- $\alpha$  in the renal tissues of rats.** The protein level of p-PKC- $\alpha$ -Thr638 in the renal tissues of Thy-1N and NRS rats at 1 h was examined by IHC staining (Magnification,  $\times 400$ ). \*\*  $P < 0.01$  vs. NRS group. Data were represented as means  $\pm$  SE (n=5 in each group).

**Figure S13**

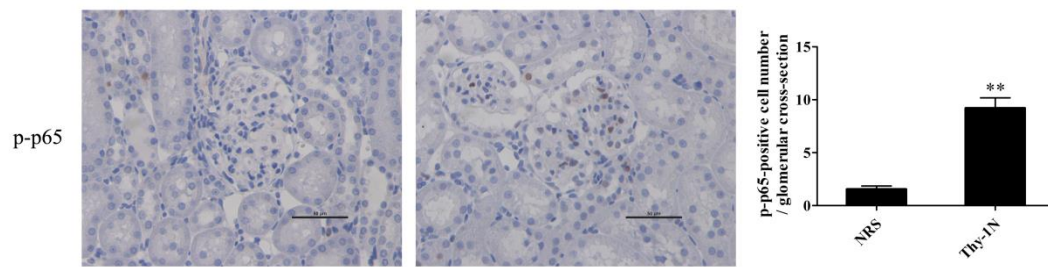
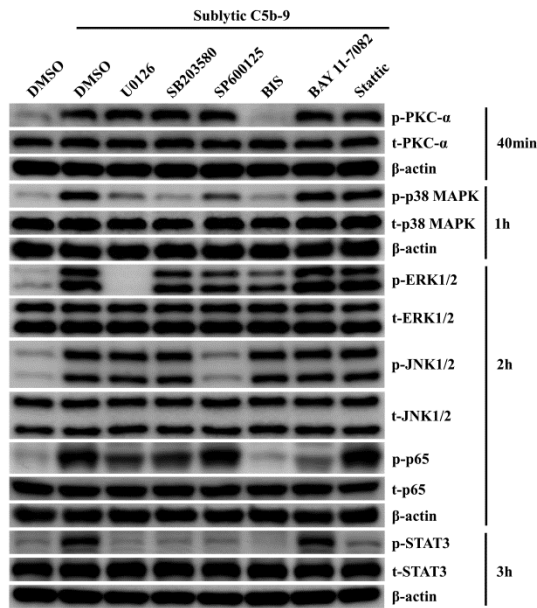


**Figure S13. The phosphorylation of p65 in the renal tissues of rats.** The protein levels of p-p65-Ser536 in the renal tissues of Thy-1N and NRS rats at 2 h were examined by IHC staining (Magnification,  $\times 400$ ). \*\*  $P < 0.01$  vs. NRS group. Data were represented as means  $\pm$  SE (n=5 in each group).

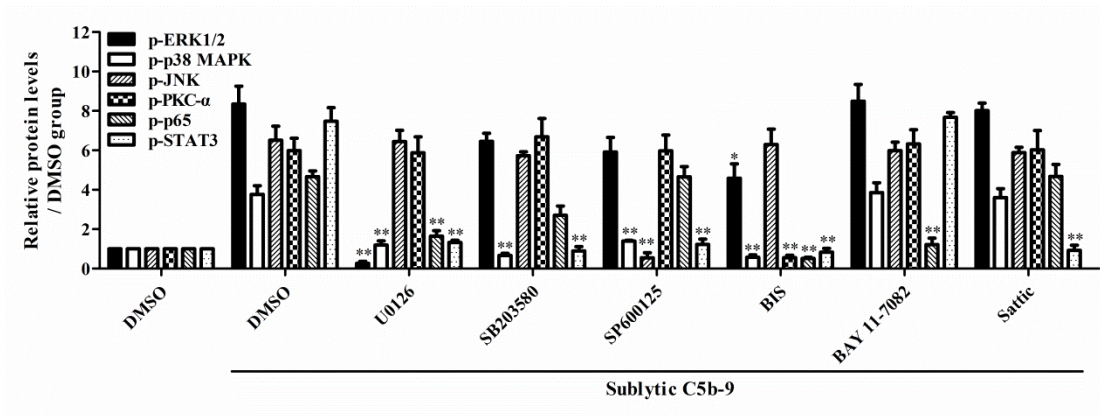


**Figure S14**

**A**



**B**



**C**

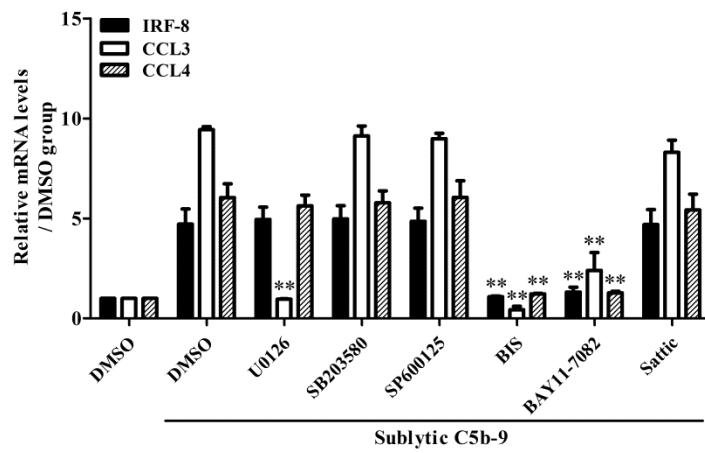


**Figure S14. The effects of different inhibitors on the corresponding protein expression and CCL3/4 production.** Rat GMCs was incubated with U0126 (ERK1/2 inhibitor, 10  $\mu$ M), SB203580 (p38 MAPK inhibitor, 10  $\mu$ M), SP600125 (JNK inhibitor, 10  $\mu$ M), BIS (PKC- $\alpha$  inhibitor, 10  $\mu$ M), BAY 11-7082 (p65 inhibitor, 10  $\mu$ M), Stattic (STAT3 inhibitor, 10  $\mu$ M) for 30 min, and then stimulated with sublytic C5b-9 for different time. The expression and phosphorylation levels of ERK1/2, p38 MAPK, JNK, PKC- $\alpha$ , p65, STAT3, IRF-8 and CCL3/4 were detected by IB (A and B) and qPCR (C). \*\* P<0.01 vs. DMSO + sublytic C5b-9 group. Data were represented as means  $\pm$  SE (n=3).

**Figure S15**

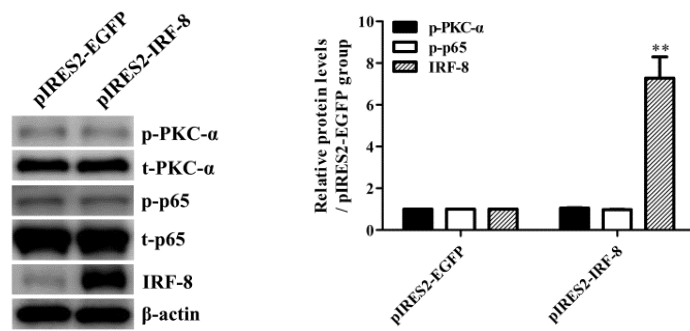


**Figure S15. The effects of IRF-8 overexpression on PKC- $\alpha$  and p65 phosphorylation.** Rat GMCs were transfected with pIRES2-IRF-8 or pIRES2-EGFP for 48 h, and then the expression and phosphorylation of IRF-8, PKC- $\alpha$  and p65 in the GMCs were detected by IB experiments. \*\*  $P < 0.01$  vs. pIRES2-EGFP group. Data were represented as means  $\pm$  SE (n=3).

**Figure S16**

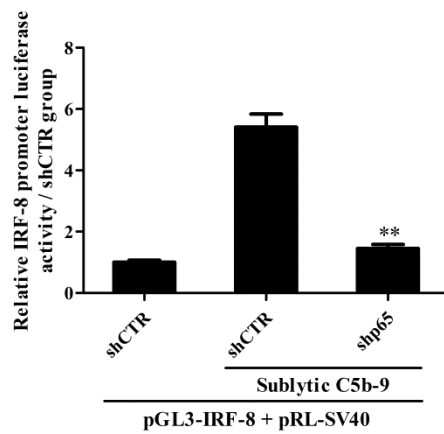


**Figure S16. The effect of p65 knockdown on IRF-8 gene transcription in the GMCs induced by sublytic C5b-9.** The plasmids of shp65, shCTR, pGL3-IRF-8 and pRL-SV40 were co-transfected into rat GMCs for 48 h in different groups followed by sublytic C5b-9 stimulation for 3 h, and then the luciferase activity was detected. Data were represented as means  $\pm$  SE (n=3). \*\* P<0.01 vs. shCTR + sublytic C5b-9.

**Figure S17**

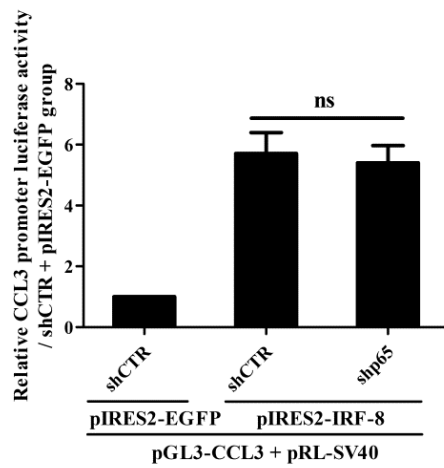


**Figure S17. The effect of p65 knockdown on CCL3 gene transcription in the GMCs induced by IRF-8 overexpression.** The plasmids of shp65, shCTR, pIRES2-IRF-8, pIRES2-EGFP, pGL3-CCL3 and pRL-SV40 were co-transfected into rat GMCs for 48 h in different groups, and then the luciferase activity was detected. Data were represented as means  $\pm$  SE (n=3). <sup>ns</sup> P>0.05.

**Figure S18**

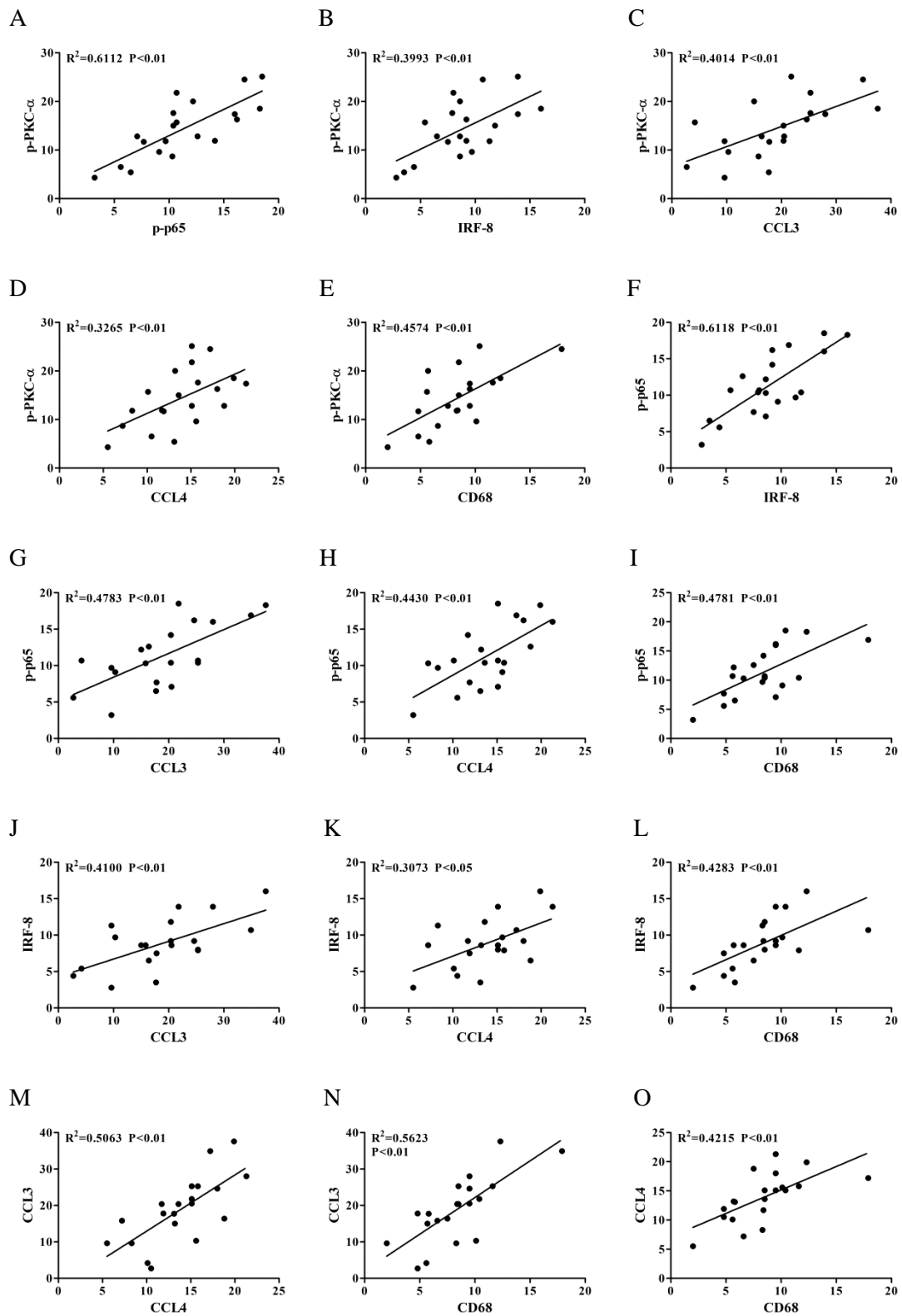


**Figure S18. Correlation analysis between p-PCK- $\alpha$ , p-p65, IRF-8, CCL3/4 and CD68 protein expression in the renal tissues of MsPGN patients.**